

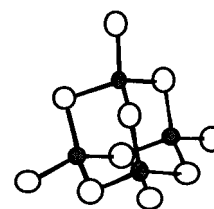
Communications

Mesostructured Non-Oxidic Solids with Adjustable Worm-hole Shaped Pores: M-Ge-Q (Q = S, Se) Frameworks Based on Tetrahedral $[\text{Ge}_4\text{Q}_{10}]^{4-}$ Clusters**

By Michael Wachhold, K. Kasthuri Rangan, Simon J. L. Billinge, Valeri Petkov, Joy Heising, and Mercouri G. Kanatzidis*

The discovery of MCM-41^[1] and its relatives^[2–4] has spawned a revolution in the design and synthesis of tailored mesostructured oxide-based materials. By comparison, non-oxidic solids such as sulfides or selenides are only very little explored—partly because of difficulties in handling or obtaining relevant precursors (e.g., $[\text{SiS}_4]^{4-}$ units). Direct sulfur and selenium analogs of MCM-41 type materials would be the thio- and seleno- aluminosilicates. However, these systems are expected to be very unstable to hydrolysis. Therefore, one needs a *working analog* for the sulfides and selenides to mimic some of the characteristics of the $[\text{SiO}_4]^{4-}$ unit. A suitable such building unit with tetrahedral topology and similar charge is the adamantane thioanion $[\text{Ge}_4\text{S}_{10}]^{4-}$ (or its selenium analog) (Scheme 1), which is made of four corner-linked $[\text{GeS}_4]^{4-}$ tetrahedra. We have already studied in detail their corresponding salts $(\text{RNMe}_3)_4[\text{Ge}_4\text{Q}_{10}]$ (abbrev. as C_nGeQ) with various surfactants.^[5] Reports on mesostructured chalcogenides have begun to appear, such as CdS ^[6] and ZnS ^[7] prepared through the incorporation of surfactants. Also, initial studies on mesostructured tin sulfides^[8] and a brief report on the synthesis of mesostructured thiogermanates resulting from the hydrothermal treatment of amorphous GeS_2 and $\text{C}_{16}\text{H}_{33}\text{NMe}_3^+\text{Br}^-$ (CTA), are noteworthy.^[9] Various microstructured metal sulfides resembling those of zeolites have been forecast^[10] and important first steps have been made

in recent years.^[11–14] The adsorption and sensing behavior of some structurally well-defined microporous lamellar tin sulfides (cation)₂Sn₃S₇ have been explored.^[15] Small guests such as NH_3 , H_2S , and alcohols were found to interact with these materials. A recent exciting development toward producing well-defined mesostructured materials is the discovery of ASU-32, a novel indium sulfide that features pore diameters of $\sim 14.5 \text{ \AA}$.^[16]



Scheme 1.

We describe here a new class of mesostructured $\text{M}/\text{Ge}_4\text{Q}_{10}$ ($\text{M} = \text{Zn}, \text{Cd}, \text{Hg}, \text{Co}$) based frameworks with large, adjustable, surfactant-filled worm-hole like tunnels. We have employed the electrostatic self-assembly approach developed at Mobil,^[1] using a mainly *aqueous* route (with methanol or ethanol added), and employing suitable cationic organic surfactant species, to form mesoporous metal sulfide frameworks. These materials are formulated as $(\text{RNMe}_3)_2[\text{MGe}_4\text{Q}_{10}]$ ($\text{Q} = \text{S}, \text{Se}$) and will be referred to as C_nMGeQ ($n = 12, 14, 16, 18$).

While this manuscript was in preparation, Ozin et al. reported on the *non-aqueous* synthesis of mesostructured metal germanium sulfides from $[\text{Ge}_4\text{S}_{10}]^{4-}$ clusters.^[17] These materials contain CTA surfactant and $\text{M}_2\text{Ge}_4\text{S}_{10}$ frameworks with hexagonally packed pores, ($\text{M} = \text{Zn}, \text{Ni}, \text{and Co}$) and $\text{M}_4\text{Ge}_4\text{S}_{10}$ ($\text{M} = \text{Cu}$). They require formamide for synthesis, and contain some water ($\sim 5 \text{ wt.}\%$). The mesostructured C_nMGeQ materials described here differ substantially from the $(\text{CTA})_2\text{M}_2\text{Ge}_4\text{S}_{10}$ systems.^[17] These differences include a) synthesis method, b) chemical formula, c) overall three-dimensional framework organization, and d) thermal stability. In addition, the $(\text{CTA})_2\text{M}_2\text{Ge}_4\text{S}_{10}$ systems are described to possess a “highly flexible and adjustable composition”, as opposed to the rigid and definitive stoichiometry that we find in C_nMGeQ .

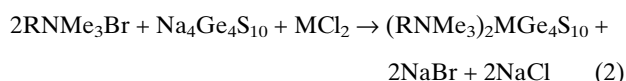
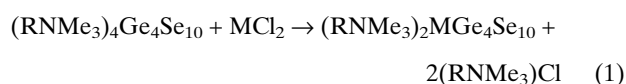
Using metathesis reactions between the $[\text{Ge}_4\text{Q}_{10}]^{4-}$ ($\text{Q} = \text{S}, \text{Se}$) anions and metal dichlorides in the presence of long chain cationic surfactant molecules, we synthesized a number of C_nMGeQ ($n = 12, 14, 16, 18$) compounds with the divalent metal ions $\text{Zn}, \text{Cd}, \text{Hg}, \text{and Co}$ ^[18] in water/methanol or water/ethanol mixtures. The products can be obtained between $20\text{--}80^\circ\text{C}$, either by mixing C_nGeQ and MCl_2 , or $\text{A}_4\text{Ge}_4\text{Q}_{10}$ ($\text{A} = \text{Na}, \text{K}$), MCl_2 salts, and $\text{C}_n\text{H}_{2n+1}\text{NMe}_3\text{Br}$, see Equations 1 and 2. The sulfides are white (Zn and Cd) or yellow (Hg), whereas the selenides

[*] Prof. M. G. Kanatzidis, Dr. M. Wachhold, Dr. K. K. Rangan, Dr. J. Heising
Department of Chemistry and Center for Fundamental Materials Research
Michigan State University
East Lansing, MI 48824 (USA)

Prof. S. J. L. Billinge, Dr. V. Petkov
Department of Physics and Astronomy and Center for Fundamental Materials Research
Michigan State University
East Lansing, MI 48824 (USA)

[**] Financial support from the National Science Foundation CHE 96-33798, (Chemistry Research Group) is gratefully acknowledged. Part of this work was carried out using the facilities of the Center for Electron Optics of Michigan State University. We acknowledge the use of the W. M. Keck Microfabrication Facility at Michigan State University, a NSF MRSEC facility. M.W. thanks the Deutsche Forschungsgemeinschaft for a postdoctoral research fellowship. We thank Professor T. J. Pinnavaia for fruitful discussions.

are generally darker (yellow for Zn, Cd, brownish for Hg). On the other hand the Co phases are dark green (S) or almost black (Se). These materials have a reproducible and consistent composition corresponding to the formula $(\text{RNMe}_3)_2[\text{MGe}_4\text{Q}_{10}]$ and form over a wide $[\text{Ge}_4\text{Q}_{10}]^{4-}/\text{MCl}_2$ ratio. They are stoichiometric compounds in which the charge on the $[\text{Ge}_4\text{Q}_{10}]^{4-}$ cluster is balanced by one M^{2+} and two surfactant RNMe_3^+ ions. The elemental composition was determined with energy dispersive microprobe analysis (EDS), which consistently gave a M:Ge:Q ratio of 1:4:10. Interestingly, the methods used to obtain C_nMGeQ did not yield the corresponding phases with Mn^{2+} ions.^[19]



It comes as a surprise to us that the formamide-made materials reported by Ozin et al. have a different stoichiometry, namely $(\text{C}_{16}\text{H}_{33}\text{NMe}_3)_2\text{M}_2\text{Ge}_4\text{S}_{10}$ (for M = Zn, Ni) and $(\text{C}_{16}\text{H}_{33}\text{NMe}_3)_2\text{M}_4\text{Ge}_4\text{S}_{10}$ (for M = Cu).^[17] Charge balancing considerations imply the presence of reduced metal ions such as Zn^{1+} , Ni^{1+} (or M^{2+}/M^0 mixtures) and Cu^0 . Barring any occluded anionic species going undetected, the cause of these unprecedented formulae is unclear.

The three-dimensional organization of C_nMGeQ was explored with X-ray scattering, infrared (IR) and Raman spectroscopy and thermal analysis. Structural characterization was carried out using low- and wide-angle X-ray diffraction (XRD), pair distribution function (PDF) analysis and high-resolution transmission electron microscopy (HRTEM).

A very strong and relatively sharp peak in the low-angle region of the diffraction pattern reveals the mesostructured nature of C_nMGeQ . Figure 1A shows a representative XRD pattern from the mesostructured phase $\text{C}_{14}\text{CdGeS}$

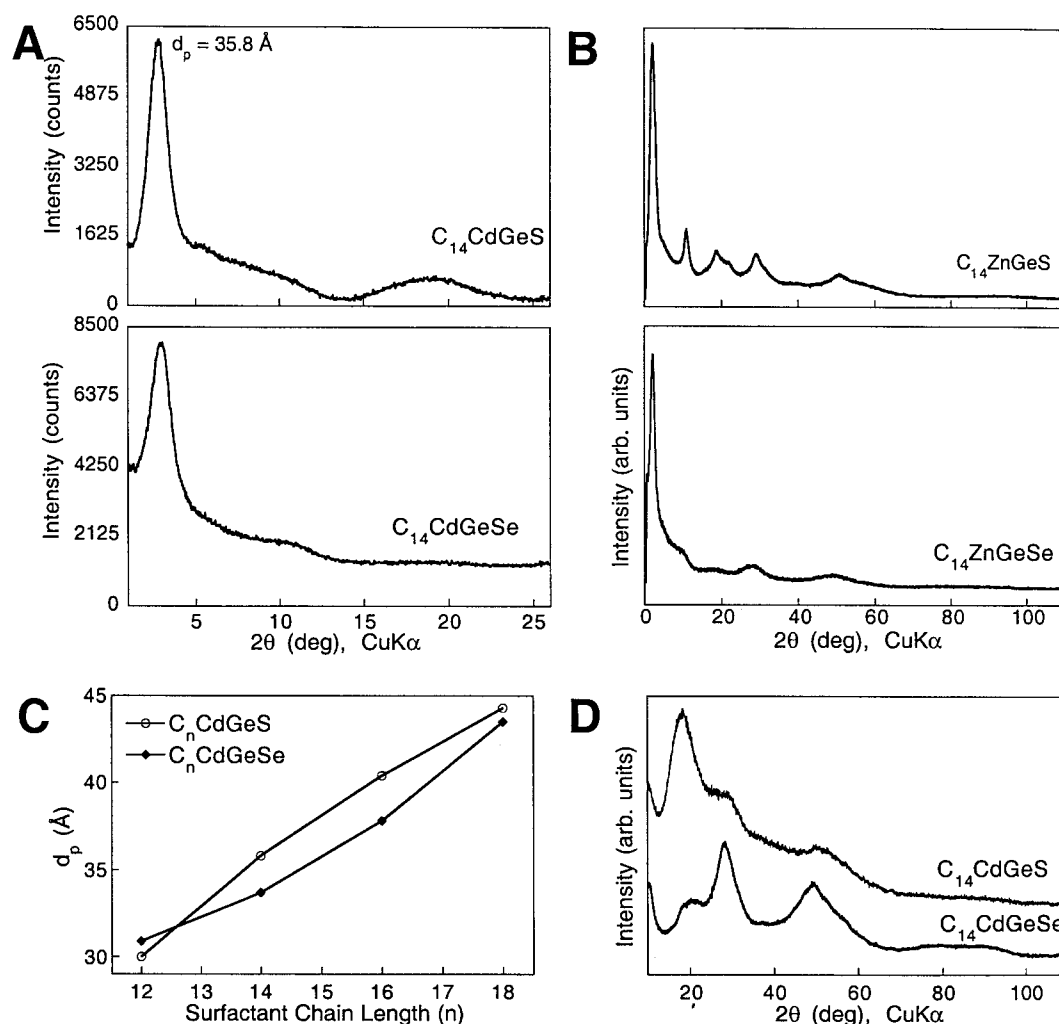


Fig. 1. A) Low-angle region of the XRD pattern of mesostructured $\text{C}_{14}\text{CdGeQ}$ (Q = S, Se). The peak maxima correspond to d -spacings of ca. 36 Å and 34 Å, respectively, which express the average pore–pore separation (d_p) in these materials. B) Full XRD pattern of the $\text{C}_{14}\text{ZnGeQ}$ (Q = S, Se) phases ($2\theta = 0\text{--}110^\circ$). C) Pore spacings as a function of surfactant chain length n in C_nCdGeQ ($n = 12, 14, 16, 18$; Q = S, Se), showing an almost linear relationship. D) Wide-angle diffuse scattering for $\text{C}_{14}\text{CdGeQ}$.

and $C_{14}CdGeSe$. Similar peaks are observed in many mesostructured silicates, aluminophosphates and other metal oxides where the d -spacing indicates the average mesopore separation.^[20,21] Figure 1B shows the low-angle portion of typical powder patterns for $C_{14}ZnGeS$ and $C_{14}ZnGeSe$. The Hg and Co analogs show very similar patterns. In the present samples the d -spacing is adjustable and increases with increasing surfactant chain length from ~ 30 Å for C_{12} to >40 Å for C_{18} surfactants (Fig. 1C). MCM-41 exhibits higher-order reflections because the pores in them form a regular hexagonal packing arrangement.^[1] In contrast, the C_nMGeS and C_nMGeSe materials do not show such reflections, which implies the absence of regular pore packing with intermediate range order, and in this sense they are more akin to the MSU-1/-2/-3 silicas.^[22]

The absence of sharp Bragg diffraction peaks in the powder XRD pattern means that the framework “walls” have no long-range order. However, these materials exhibit well-defined diffuse scattering (at $2\theta > 10^\circ$), which is consistent with the presence of short-range local order and non-periodic wall structure much like the wall structure of mesoporous silicas. The surfactant-filled tunnels are then organized like worm holes, at the same time keeping a constant average tunnel to tunnel distance to be expressed as a strong low-angle peak in the diffraction pattern.

The position and intensity of the low-angle peak in the XRD pattern is almost insensitive to temperature, suggesting that the overall structure of the $[MGe_4Q_{10}]^{2-}$ framework in C_nMGeQ is neither one- nor two-dimensional. In low-dimensional systems large changes in the surfactant chain conformation should cause large changes in the low-angle diffraction peak as a function of temperature. Instead in C_nMGeQ the high d -spacing peaks move only very little with temperature and survive even after the materials have lost most of their surfactant at $220^\circ C$ (see below). Differential scanning calorimetry does not show any phase transitions of the type typically observed in lamellar phases. Such transitions arise from the “melting” or rearrangement of the long surfactant chains in the intralamellar space (liquid-crystal behavior). By comparison, the precursor phases C_nGeQ , which are lamellar, exhibit prominent transitions at 120 – $160^\circ C$.^[5] This strongly suggests that C_nMGeQ phases have rigid three-dimensional, non-periodic, mesostructured frameworks. Furthermore, absolutely no swelling (or dissolution) was observed with C_nMGeQ upon exposure to a large number of solvents (e.g., many n -alcohols, n -amines, dimethylformamide, acetonitrile, acetone, benzene, nitromethane, etc.) as judged by the position of the high d -spacing peak. One- or two-dimensional systems separated by long surfactant chains are subject to swelling in the presence of suitable polar solvents, as, for example, the “precursor” lamellar phases C_nGeQ .^[5]

Wide-angle X-ray scattering data for $C_{14}CdGeQ$ are shown in Figure 1D. The diffuse scattering pattern remains similar on changing the length of the surfactant molecule and shows small differences on changing the metal bridging

ion. This suggests that the local structure adopted by the transition metal is similar in all phases and that the diffuse scattering comes predominantly from the same structural building block that is the adamantoid $[Ge_4Q_{10}]^{4-}$ itself. Direct evidence for this is obtained by atomic-pair distribution functions (PDFs).

The reduced structure factors for $C_{14}ZnGeQ$ obtained from the powder diffraction data are shown in Figure 2A.^[23] The PDFs show that the short-range order is well defined, suggesting the presence of structurally rigid, well-defined fragments (see Fig. 2B). The assignment of characteristic atom-pairs at $\sim 2.2(2.4)$ Å and $\sim 3.8(4.0)$ Å correspond to the Ge–S(Se) and Ge–Ge vectors in the $[Ge_4Q_{10}]^{4-}$ cluster, consistent with the presence of this building block in the framework. The structural coherence is virtually gone by 10 Å, which is approximately the M–M separation. This suggests that long-range order is destroyed due to lack of well-defined orientational relationship between neighboring adamantoid ions. The metal ions connecting the adamantoid ions are acting as hinges (see Fig. 2C). We estimate that these $[MGe_4Q_{10}]^{2-}$ frameworks are able to enclose a circle with a diameter between 20 – 30 Å using between six and ten stoichiometric units (depending on surfactant), only changing their positions relative to each other, but not the connectivities. Details of the structural modeling will be reported elsewhere.^[24]

Additional support for the structural model comes from HRTEM photographs, which reveal that the samples have disordered, worm-hole-like features (see Fig. 3A) that resemble examples for disordered mesoporous oxides.^[25] The tunnel dimensions are roughly 22 – 32 Å and there is a significant degree of disorder, consistent with the X-ray powder diffraction results.

The Raman and IR spectra of all C_nMGeQ phases show that the adamantane cluster remains intact. They also give evidence for additional M–Q bonds associated with the terminal chalcogenide ions of the adamantane cluster. Figure 4A shows the Raman scattering from corresponding sulfide and selenide phases in the region 75 – 500 cm^{-1} . They are representative examples as the spectra of other C_nMGeQ compounds with different n and M are very similar. The comparison of these spectra with those of the precursor compounds C_nGeQ ^[5] or corresponding compounds^[26]—where the $[M_4Q_{10}]^{4-}$ (M = Ge, Sn; Q = S, Se) units remain free of linkage metal atoms—shows mainly that the vibration modes of the inner Ge_4Q_6 cage are not substantially affected through the linkage of the cluster (Fig. 4A). The modes involving the terminal chalcogenido atoms, however, are considerably influenced. The metal coordination causes the ν_1 modes of the terminal Ge–Q bonds, at 460 cm^{-1} for the S and at 315 cm^{-1} for the Se analogs, to red-shift by 10 cm^{-1} and 15 cm^{-1} respectively, compared to the spectra of the uncoordinated clusters. These bands are strongly suppressed, and furthermore, in the area of 380 – 460 cm^{-1} for C_nMGeS and 230 – 340 cm^{-1} for C_nMGeSe a broader low-intensity peak occurs. This broad-

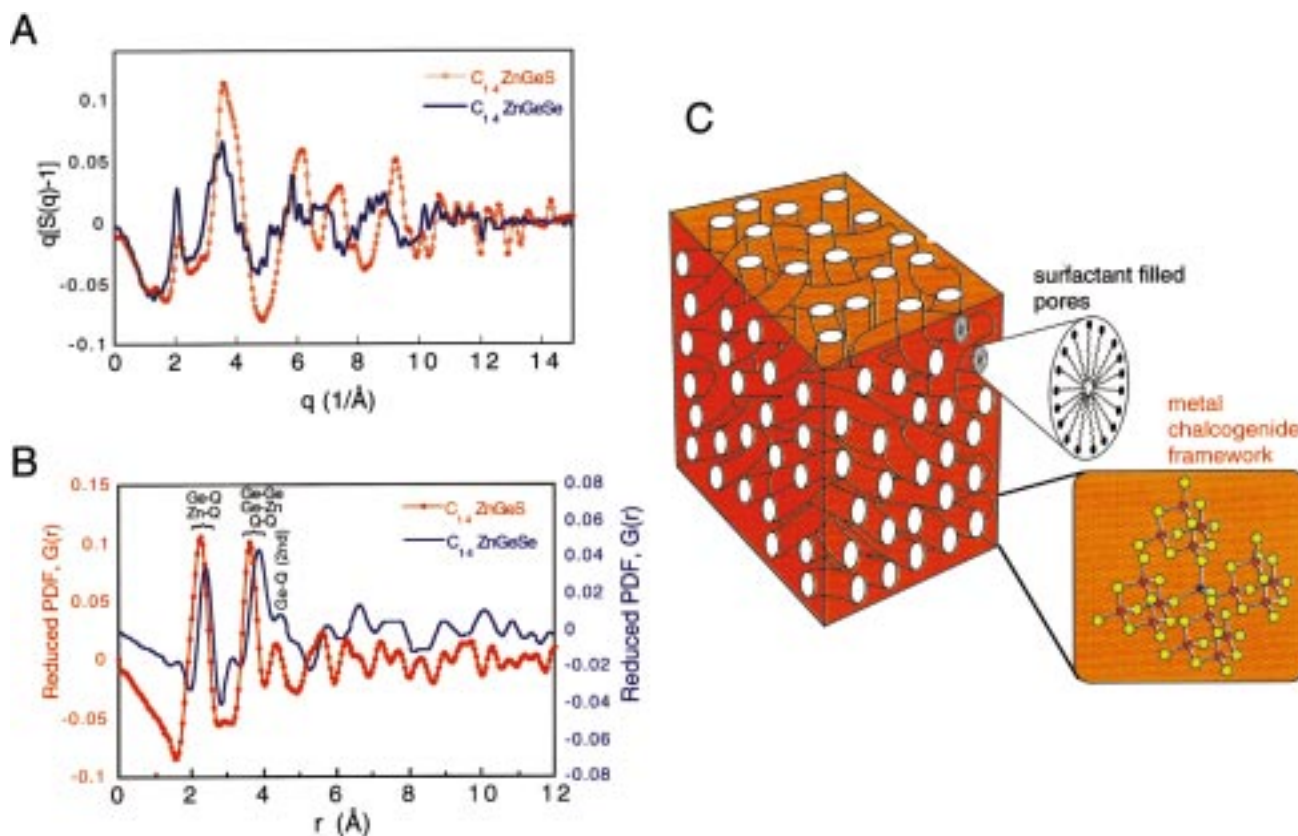


Fig. 2. A) Reduced structure factors $q[S(q)-1]$ for $C_{14}ZnGeQ$ ($Q = S, Se$). B) The corresponding PDFs. The labeled peaks are interatomic pair correlations associated with the presence of the $[Ge_4Q_{10}]^{4+}$ cluster. C) Schematic depiction of worm-hole-like morphology in the mesostructured covalent $3_2[MGe_4Q_{10}]^{2-}$ framework. The surfactant molecules occupy the framework pores. Yellow circles are S(Se) atoms, red circles are Ge atoms and blue circles are M atoms.

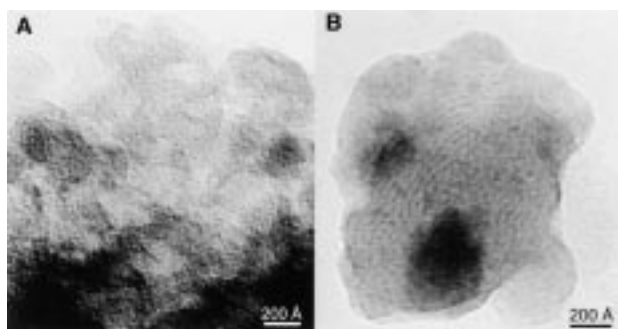


Fig. 3. A) HRTEM image of as prepared $C_{14}CdGeSe$. B) HRTEM image of “calcined” $C_{14}CdGeSe$ (“calcination” temperature $\sim 190^\circ C$). The meso-scaled worm-hole-like features remain intact after the “calcination” process. The samples were examined at 120kV on a JEOL 120CX TEM. A carbon-supported copper grid was dipped in the dry powder or in a suspension of the sample in hexane.

ening is understood in terms of the non-periodic character of the structure of the $[MGe_4Se_{10}]^{2-}$ framework.^[27]

An important difference between the extensively investigated silicate or other oxidic mesostructured materials and the chalcogenido materials described here is the considerably narrower-energy bandgap of the latter. Solid-state UV-vis spectroscopy shows that the compounds with Zn, Cd and Hg possess well-defined, sharp optical absorptions associated with bandgap transitions in the energy range 1.6–3.4 eV, (see Fig. 4B). This makes these mesostructured

chalcogenides potentially interesting for a number of unique electronic and photonic applications. Within the same chalcogenide family (e.g., Zn, Cd, Hg), the lowest-energy bandgap occurs in the Hg analogs. On the other hand, for a given metal, the bandgaps are independent of the surfactant chain length (Fig. 4B, bottom). The optical spectra of the Co^{2+} compounds are dramatically different and show intense optical S→Co charge transfer transitions as well as d–d transitions^[28] (333, 717 and 1741 nm).

Thermal gravimetric analysis (TGA) of C_nMGeQ materials show that they lose all their surfactant molecules between 150 and 400 °C (Fig. 4C). In all cases the measured values correspond to two surfactant molecules per adamantane unit. Mass spectroscopic analysis confirms the presence of species such as NMe_3^+ , $RNMe_2^+$ among others. At 400 °C the materials decompose to amorphous GeS_2 and crystalline MS or crystalline $GeSe_2$ and MSe. Unlike the formamide synthesized materials^[17] we see no evidence for the presence of water. The IR spectra do not show the typical water absorptions at $\sim 3500\text{ cm}^{-1}$ and 1600 cm^{-1} .

Based on the TGA experiments we have attempted to remove the organic component by heat treatment, a step analogous to the air calcination used to remove the surfactant template molecules for micro- and mesoporous oxides. The major difference in the procedure is that the mesostructured chalcogenides were heated under dynamic vac-

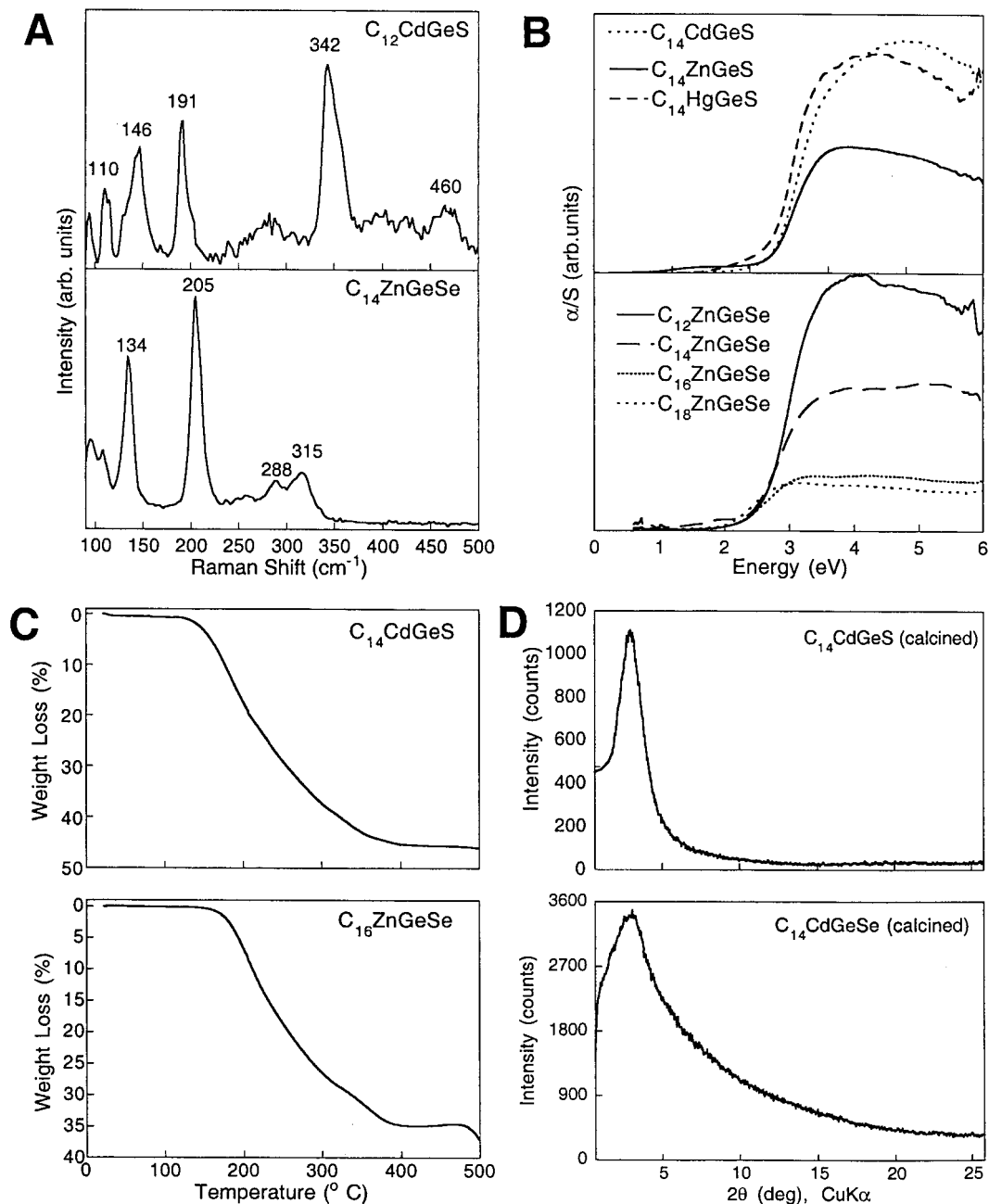


Fig. 4. A) Raman spectra of C₁₂CdGeS and C₁₄ZnGeSe. Spectra were recorded on a Holoprobe Raman spectrograph equipped with a 633 nm Helium–Neon laser and a CCD camera detector. The instrument was coupled to an Olympus BX60 microscope. B) Optical absorption spectra of C_nZnGeQ (*n* = 12, 14, 16, 18; Q = S, Se). UV-vis–near IR diffuse reflectance spectra were obtained at room temperature on a Shimadzu UV-3101PC double-beam, double-monochromator spectrophotometer (200 > λ > 2500 nm). The instrument is equipped with an integrating sphere. BaSO₄ powder was used as a reference (100 % reflectance) and base material, in which the ground sample was coated. Reflectance data were converted to absorbance as described by McCarthy et al. [29]. C) TGA analyses of C₁₄CdGeS and C₁₆ZnGeSe. The total weight loss at 450 °C corresponds to the general formula (RNMe₃)₂M-Ge₄Q₁₀. Combined TGA/mass spectroscopy analysis of the evolved volatile products show RNMe₂ and NMe₃ and their decomposition products. D) X-ray powder diffraction diagrams of “calcined” C₁₄CdGeQ (Q = S, Se) samples. The low-angle peaks corresponds to ~31 Å for both materials.

um and at much lower temperatures than the oxides. We chose “calcination” temperatures at around 180–220 °C—typically at the inflection point of the weight-loss curves. We find that about 70–80 % of the organic part can be removed, *without collapse* of the framework, after heating under vacuum for 3–4 days. Again this is in sharp contrast

with what is observed in the CTA/M₂Ge₄S₁₀ systems, which reportedly lose 30–40 % of their surfactant species at ~300 °C. In the “calcined” mesostructured materials, the low-angle, high *d*-spacing peak remains prominent in the diffraction pattern, though it shifts slightly to higher angles, which indicates a decrease in the mesopore spacing of typi-

cally $\sim 3\text{--}5 \text{ \AA}$ (Fig. 4D). At the same time, the high-angle region of the XRD patterns unambiguously shows that the frameworks remain essentially intact, with only a slight modification of the shape of the diffuse scattering. This suggests that the structure of the “calcined” products mirrors that of their C_nMGeQ precursors. In fact, “calcined” samples appear by HRTEM to have worm-hole-like features with widths of $25\text{--}35 \text{ \AA}$ (Fig. 3B), in a similar fashion to their precursors discussed above. We were not able to measure any absorption properties using N_2 and water. Since about 20 % of the surfactant remains inside the framework it serves as a blocking agent preventing access to the pores. The same problem was encountered in CTA/ $M_2Ge_4S_{10}$ materials. An appropriate method for the complete removal of the surfactant molecule must first be devised before the absorption properties of these frameworks can be exploited.

In conclusion, a new family of mesostructured compounds with the general formula $(C_nH_{2n+1}NMe_3)_2[MGe_4Q_{10}]$ ($M = Zn, Cd, Hg, Co$; $Q = S, Se$; $n = 12, 14, 16, 18$) and adjustable pore size has been synthesized and characterized. These materials possess an amorphous, three-dimensional framework structure $^3[MGe_4Q_{10}]^{2-}$ in which simple adamantane clusters are the basic building blocks. It appears that the selection of the solvent plays a major role in these systems. The use of formamide leads to a hexagonally ordered pore structure (and a different stoichiometry), whereas H_2O /alcohol mixtures favor disordered pore structures with worm-hole character. The surfactant molecules occupy the tunnels that bore through this framework in a worm-hole-like manner. The compounds lose $\sim 70 \%$ of their surfactant molecules when heated up to $220 \text{ }^\circ\text{C}$ without framework collapse. All compounds are wide bandgap semiconductors, the Se phases showing lower values than the sulfide analogs. Such structures may find applications in shape selective electro- and photocatalysis, or in environmental remediation of heavy metals and chemoselective sensing.

Received: April 28, 1999
Final version: August 10, 1999

- [1] C. T. Kresge, M. E. Leonowicz, W. J. Roth, J. C. Vartuli, J. S. Beck, *Nature* **1992**, 359, 710. J. S. Beck, J. C. Vartuli, W. J. Roth, M. E. Leonowicz, C. T. Kresge, K. D. Schmitt, C. T.-W. Chu, D. H. Olson, E. W. Sheppard, S. B. McCullen, J. B. Higgins, J. L. Schlenker, *J. Am. Chem. Soc.* **1992**, 114, 10834.
- [2] P. D. Yang, T. Deng, D. Y. Zhao, P. Y. Feng, D. Pine, B. F. Chmelka, G. M. Whitesides, G. D. Stucky, *Science* **1998**, 282, 2244. Q. S. Hue, D. I. Margolese, U. Ciesla, P. Y. Feng, T. E. Gier, P. Sieger, R. Leon, P. M. Petroff, F. Schuth, G. D. Stucky, *Nature* **1994**, 368, 317.
- [3] P. T. Tanev, T. J. Pinnavaia, *Science* **1996**, 271, 1267. P. T. Tanev, M. Chibwe, T. J. Pinnavaia, *Nature* **1994**, 368, 321.
- [4] S. A. Davis, S. L. Burkett, N. H. Mendelson, S. Mann, *Nature* **1997**, 385, 420. C. E. Fowler, S. L. Burkett, S. Mann, *Chem. Commun.* **1997**, 1769.
- [5] F. Bonhomme, M. G. Kanatzidis, *Chem. Mater.* **1998**, 10, 1153. M. Wachhold, M. G. Kanatzidis, unpublished.
- [6] P. Osenar, P. V. Braun, S. I. Stupp, *Adv. Mater.* **1996**, 8, 1022. P. V. Braun, P. Osenar, S. I. Stupp, *Nature* **1996**, 380, 325. S. I. Stupp, P. V. Braun, *Science* **1997**, 277, 1242.
- [7] J. Li, H. Kessler, M. Souillard, L. Khouchaf, M.-H. Tuilier, *Adv. Mater.* **1998**, 10, 946.
- [8] T. Jiang, G. A. Ozin, *J. Mater. Chem.* **1998**, 8, 1099. T. Jiang, G. A. Ozin, R. L. Bedard, *J. Mater. Chem.* **1998**, 8, 1641.
- [9] M. Fröba, N. Oberender, *Chem. Commun.* **1997**, 1729.
- [10] R. L. Bedard, S. T. Wilson, L. D. Vail, J. M. Bennett, E. M. Flanigen, in *Zeolites: Facts, Figures, Future* (Eds: P. A. Jacobs, R. A. van Santen) Elsevier, B. V., Amsterdam, Netherlands **1989**, vol. 1, pp. 375–387. R. L. Bedard, L. D. Vail, S. T. Wilson, E. M. Flanigen, *U.S. Patent* 4880761 **1989**.
- [11] G. A. Ozin, *Adv. Mater.* **1995**, 7, 335. H. Ahari, C. L. Bowes, T. Jiang, T. Lough, A. Lough, G. A. Ozin, R. L. Bedard, S. Petrov, D. Young, *Adv. Mater.* **1995**, 7, 375.
- [12] O. M. Yaghi, Z. Sun, D. A. Richardson, T. L. Groy, *J. Am. Chem. Soc.* **1994**, 116, 807.
- [13] S. Dhingra, M. G. Kanatzidis, *Science* **1992**, 258, 1769. K.-W. Kim, M. G. Kanatzidis, *J. Am. Chem. Soc.* **1992**, 114, 4878. K. W. Kim, M. G. Kanatzidis, *J. Am. Chem. Soc.* **1998**, 120, 8124. A. Loose, W. S. Sheldrick, *Z. Naturforsch. B*, **1997**, 52, 687.
- [14] C. L. Cahill, J. B. Parise, *Chem. Mater.* **1997**, 9, 807. J. B. Parise, *Science* **1991**, 251, 293. J. B. Parise, K. Tan, *Chem. Commun.* **1996**, 1687. C. L. Bowes, A. J. Lough, A. Malek, G. A. Ozin, S. Petrov, D. Young, *Chem. Ber.* **1996**, 129, 283.
- [15] C. L. Bowes, W. U. Huynh, S. J. Kirkby, A. Malek, G. A. Ozin, S. Petrov, M. Twardowski, D. Young, R. L. Bedard, R. Broach, *Chem. Mater.* **1996**, 8, 2147. T. Jiang, G. A. Ozin, A. Verma, R. L. Bedard, *J. Mater. Chem.* **1998**, 8, 1649.
- [16] H. L. Li, A. Laine, M. O’Keeffe, O. M. Yaghi, *Science* **1999**, 283, 1145.
- [17] M. MacLachlan, N. Coombs, G. A. Ozin, *Nature* **1999**, 397, 681.
- [18] $(RNMe_3)_2[MGe_4S_{10}]$ ($M = Zn, Cd, Hg, Co$). $(RNMe_3)_2[MGe_4S_{10}]$ phases were prepared in ethanol/ H_2O (5:1 by volume) solutions at room temperature; the surfactants (1 mmol) were dissolved in ethanol/ H_2O (200 mL; 50:50). $Na_4Ge_4S_{10}$ (0.35 g, 0.5 mmol) was dissolved in distilled water (20 mL). MCl_2 (0.5 mmol) was dissolved in distilled water (20 mL) and the $Na_4Ge_4S_{10}$ and MCl_2 solutions were added simultaneously to the surfactant solution under constant stirring to form a copious precipitate. The mixture was stirred for 3 h at room temperature, then filtered, washed with water and vacuum-dried overnight. The yields of the colorless (Zn, Cd), yellow (Hg) yellow-brownish (Ni) or green (Co) precipitates was typically 50 % in all cases, based on $Na_4Ge_4S_{10}$. Elemental analysis coupled with thermal gravimetric analysis was reproducible, and consistent with the chemical formula $(RNMe_3)_2[MGe_4Se_{10}]$. Preparation of $(RNMe_3)_2[MGe_4Se_{10}]$ ($M = Zn, Cd, Hg, Co$): Method (a): By a 1:1 reaction of $(RNMe_3)_4Ge_4Se_{10}$ phases with corresponding metal chlorides. The $(RNMe_3)_4Ge_4Se_{10}$ phases are accessible through a stoichiometric reaction of $K_4Ge_4Se_{10}$ and $RNMe_3Br$. $(RNMe_3)_4Ge_4Se_{10}$ is dissolved in a warm ($\sim 60^\circ\text{C}$) ethanol/water mixture ($\sim 20\text{ mL}$; 1:1). A solution of MCl_2 in ethanol/water is then added dropwise to the stirred $(RNMe_3)_4Ge_4Se_{10}$ solution to give instantly a yellow (Zn, Cd) or yellow-brownish (Hg, Co) precipitate. The resulting suspension was stirred for another hour, followed by product isolation by centrifugation and subsequent decanting of the solvent. The product was washed with water and acetone to remove all residues of the surfactant salt, and dried with ether. The yield was typically $>90 \%$. Elemental analysis coupled with thermal gravimetric analysis indicated the formula $(RNMe_3)_2[MGe_4Se_{10}]$. Method (b): $K_4Ge_4Se_{10}$ and two equivalents of $R-NMe_3Br$ were dissolved in $H_2O/MeOH$ ($\sim 20 \text{ mL}$; 1:1) and heated to $50\text{--}60 \text{ }^\circ\text{C}$ to give a yellow solution. The solution of the MCl_2 salt in H_2O (10 mL) was slowly added to this mixture under vigorous stirring, which lead to immediate precipitation of the product. The isolation and purification was the same as for method (a). The C_nMGeQ materials are insoluble in all common solvents such as H_2O , alcohols or acetone.
- [19] K. K. Rangan, M. Wachhold, M. G. Kanatzidis, unpublished.
- [20] A. Taguchi, T. Abe, M. Iwamoto, *Microporous Mater.* **1998**, 21, 387. M. S. Wong, J. Y. Ying, *Chem. Mater.* **1998**, 10, 2067. A. Taguchi, T. Abe, M. Iwamoto, *Adv. Mater.* **1998**, 10, 667.
- [21] K. G. Severin, T. M. Abdel-Fattah, T. J. Pinnavaia, *Chem. Commun.* **1998**, 1471.
- [22] E. Prouzet, T. J. Pinnavaia, *Angew. Chem. Int. Ed. Engl.* **1997**, 36, 516. S. A. Bagshaw, T. J. Pinnavaia, *Angew. Chem. Int. Ed. Engl.* **1996**, 35, 1102. W. Z. Zhang, T.R. Pauly, T. J. Pinnavaia, *Chem. Mater.* **1997**, 9, 2491.
- [23] The XRD data for the atomic Pair Distribution Function (PDF) determination were collected independently using a Huber diffractometer in symmetric reflection geometry ($2\theta_{\text{max}} \leq 140^\circ$) and $MoK\alpha$ radiation ($\lambda = 0.7107 \text{ \AA}$). The data were corrected for background, absorption, Polarization, Compton and multiple scattering. The data were then normalized by the incident flux, the number of scatterers and the ave-

rage atomic form factor of the sample to obtain the normalized total scattering function $S(q)$ ($q = 4\pi\sin\theta/\lambda$ where 2θ is the scattering angle). The reduced radial distribution function, or pair distribution function, is obtained from $S(Q)$ through a Fourier transform:

$$S(q) = N[f_{\text{ave}}(q)]^2 \left[1 + \int_{-\infty}^{\infty} 4\pi r^2 \rho(r) \frac{\sin qr}{qr} dr \right]$$

$$G(r) = [4\pi r^2 \rho(r) - 4\pi r^2 \rho_0] = \frac{2r}{\pi} \int_0^{\infty} q [s(q)] \sin(rq) dq$$

where: f_{ave} = average atomic scattering factor, Z = atomic number, N = number of scattering atoms, $\rho(r)$ = atomic pair density function. The function $G(r)$ represents the radial density distribution showing peaks at distances, r , which separate pairs of atoms in the solid. It is a measure of the short-range atomic order in the solid and does not presume any crystallinity. The procedures used to perform PDF analysis of XRD data have been published [T. Egami, *Mater. Trans. JIM* **1990**, *31*, 163. S. J. L. Billinge, T. Egami, *Phys. Rev. B* **1993**, *47*, 14 386].

- [24] S. J. L. Billinge, V. Petkov, M. F. Thorpe, M. Lei, M. Wachhold, K. K. Rangan, M. G. Kanatzidis, unpublished.
- [25] P. T. Tanev, T. J. Pinnavaia, *Science* **1995**, *267*, 865.
- [26] a) A. Müller, B. N. Cyrin, S. J. Cyrin, S. Pohl, B. Krebs, *Spectrochim. Acta* **1976**, *32A*, 67. b) J. Campbell, D. P. DiCiommo, H. P. A. Mercier, A. M. Pirani, G. J. Schrobilgen, M. Willuhn, *Inorg. Chem.* **1995**, *34*, 6265.
- [27] Far-IR spectra of all the sulfide phases are similar and support the Raman spectra that the Ge_4S_{10} adamantane unit is intact. A band occurring at 433 cm^{-1} corresponding to Ge-S stretching is shifted to lower frequency as compared to compounds with isolated Ge_4S_{10} units, consistent with coordination to a metal center. Corresponding shifts are observed for the Se analogs. Similar spectra were also observed for $(\text{Me}_4\text{N})_2\text{MGe}_4\text{S}_{10}$ ($M = \text{Mn, Co, Fe}$). [O. Achak, J. Y. Pivan, M. Louier, D. Lotier, *J. Solid State Chem.* **1996**, *121*, 473]. The IR spectra also give proof for the presence of the surfactant molecules in all $\text{C}_n\text{MGe}_4\text{O}$ phases. The frequencies for the C-H, C-C and C-N vibrations correspond to the expected literature values.
- [28] Weaker d-d transitions are partially allowed in a tetrahedral coordination environment.
- [29] T. J. McCarthy, S.-P. Ngeyi, J.-H. Liao, D. C. De Groot, J. Schindler, C. R. Kannewurf, M. G. Kanatzidis, *Chem. Mater.* **1993**, *5*, 331.

Principle of Low-Energy Electron Beam-Induced Current Imaging for Ferroelectric Thin Films**

By Igor Lubomirsky, Tzu-Yu Wang, Konstantin Gartsman, and Oscar M. Stafsudd*

Although there are a number of methods for measuring spontaneous polarization in ferroelectrics, each has its own difficulties, especially when related to thin polycrystalline films.^[1-5] The Sawyer bridge^[6] and capacitance voltage^[7] techniques measure the current related to the change in polarization under an externally applied electric field. These

methods work well for single crystals but for thin films,^[1,2] with relatively high trap density,^[8-10] the current generated from charging and discharging traps results in inaccurate measurements.^[11] Another method tracks the pyroelectric response to a periodic temperature change (PTC). The PTC is typically controlled by a modulated laser source and provides accurate results for spontaneous polarization.^[12] The primary drawback is poor spatial resolution unless PTC is combined with scanning optical microscopy. Ferroelectric domains may be observed by scanning electron microscopy in secondary electron mode,^[13,14] however, measurements are highly ambiguous since many factors may affect image contrast.^[15]

We present a low-energy electron beam-induced current (LEEBIC) scanning electron microscopy technique where contrast appears only due to the presence of spontaneous polarization, thus combining accuracy and spatial resolution.

Electron beam-induced current (EBIC)^[16-18] mode for scanning electron microscopy measures current induced in an external circuit during electron beam scanning. The electron beam excites free carriers that are separated by an internal electric field and collected at the top and bottom of the sample through electrodes that are connected via a sensitive current detector. Thus, the EBIC image is a map of the current induced by the electron beam at every point. Because of the relatively weak internal electric fields^[13,14,19-21] and short carrier lifetimes^[22] in typical ferroelectrics, EBIC has been considered inapplicable for measuring spontaneous polarization. However, for ferroelectrics with a sufficiently high pyroelectric coefficient our novel (LEEBIC) technique can be very useful.

LEEBIC, when applied to ferroelectrics with sufficient pyroelectric coefficients, provides accurate spontaneous polarization information at very fine resolution. The low-energy electron beam produces a temperature gradient,^[15] inducing a spontaneous polarization gradient. This polarization gradient creates an electric field that drives a significant percentage of generated carriers to the electrode. The amount of collected free carriers is equivalent to an EBIC gain of 5 to 20 in BaTiO_3 and LiTaO_3 films. Results show an image resolution of $0.5\text{--}1\ \mu\text{m}$. A high degree of accuracy and resolution is obtainable due to measurement of the induced polarization gradient and this method has none of the drawbacks associated with direct polarization measurements.

We consider a thin ($d \leq 1\ \mu\text{m}$) ferroelectric film deposited on a conductive substrate and irradiated by a low-intensity electron beam (beam current $I_b \approx 1\ \text{nA}$, acceleration voltage $V_{\text{acc}} \approx 5\text{--}15\ \text{kV}$). The film surface is covered by a thin conductive layer ($<200\ \text{\AA}$ of Au or Pd), which prevents electron beam damage to the film and serves as the top electrode. The steady-state temperature, T , distribution in the ferroelectric film can be described by Equation 1, where λ is the thermal conductivity, r is the radius, z is the depth, and $g(r,z)$ is the density of heat production.

[*] Prof. O. M. Stafsudd, Dr. I. Lubomirsky, T.-Y. Wang
University of California at Los Angeles
Electrical Engineering Department
405 Hilgard, Los Angeles, CA 90095 (USA)
Dr. K. Gartsman
Weizmann Institute of Science
Rehovot 76100 (Israel)

[**] This material is based upon work supported by, or in part by, the US Army Research Office under contract/grant number DAAH04-96-1-0389. I.L. expresses his gratitude for the support of the Rueff-Wormster Postdoctoral Fellowship.